



저작자표시-비영리-변경금지 2.0 대한민국

이용자는 아래의 조건을 따르는 경우에 한하여 자유롭게

- 이 저작물을 복제, 배포, 전송, 전시, 공연 및 방송할 수 있습니다.

다음과 같은 조건을 따라야 합니다:



저작자표시. 귀하는 원저작자를 표시하여야 합니다.



비영리. 귀하는 이 저작물을 영리 목적으로 이용할 수 없습니다.



변경금지. 귀하는 이 저작물을 개작, 변형 또는 가공할 수 없습니다.

- 귀하는, 이 저작물의 재이용이나 배포의 경우, 이 저작물에 적용된 이용허락조건을 명확하게 나타내어야 합니다.
- 저작권자로부터 별도의 허가를 받으면 이러한 조건들은 적용되지 않습니다.

저작권법에 따른 이용자의 권리는 위의 내용에 의하여 영향을 받지 않습니다.

이것은 [이용허락규약\(Legal Code\)](#)을 이해하기 쉽게 요약한 것입니다.

[Disclaimer](#)

Master's Thesis
석사 학위논문

Optimal Design of Parallel Elastic Actuator (PEA) with Spiral Spring for Wire-Tension Control

Kyeongsik Shin(신 경 식 申 炘 識)

Department of
Robotics Engineering

DGIST

2021

Optimal Design of Parallel Elastic Actuator (PEA) with Spiral Spring for Wire-Tension Control

Advisor: Professor Sehoon Oh
Co-advisor: Professor Dongwon Yun

by

Kyeongsik Shin
Department of Robotics Engineering
DGIST

A thesis submitted to the faculty of DGIST in partial fulfillment of the requirements for the degree of Master of Science in the Department of Robotics Engineering. The study was conducted in accordance with Code of Research Ethics¹

12. 28. 2020

Approved by

Professor Sehoon Oh
(Advisor)

(signature)


Professor Dongwon Yun
(Co-Advisor)

(signature)



¹ Declaration of Ethical Conduct in Research: I, as a graduate student of DGIST, hereby declare that I have not committed any acts that may damage the credibility of my research. These include, but are not limited to: falsification, thesis written by someone else, distortion of research findings or plagiarism. I affirm that my thesis contains honest conclusions based on my own careful research under the guidance of my thesis advisor.

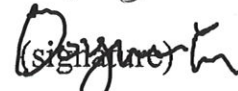
Optimal Design of Parallel Elastic Actuator (PEA) with Spiral Spring for Wire-Tension Control

Kyeongsik Shin

Accepted in partial fulfillment of the requirements for the degree of
Master of Science.

12. 28. 2020

Head of Committee Prof. Sehoon Oh (signature) 

Committee Member Prof. Dongwon Yun (signature) 

Committee Member Prof. Hae-Won Park (signature) 

MS/RT
201923010

신 경 식. Kyeongsik Shin. Optimal Design of Parallel Elastic Actuator (PEA) with
Spiral Spring for Wire-Tension Control. Department of Robotics Engineering. 2021.
v+33p. Advisors Prof. Sehoon Oh, Co-Advisors Prof. Dongwon Yun.

ABSTRACT

This study proposes a novel actuator that can generate desired tension by torque control to provide necessary load for physical exercise. In order to reduce the required torque level of the motor, a spring is incorporated in this actuator design such that the torque (and thus tension) can be generated not only by the motor but also from the spring.

The proposed mechanism is a type of the Parallel Elastic Actuator (PEA), which consists of the motor, the spring and the reduction gear. Dynamic model and analysis of PEA are developed in this paper to properly understand the working principle of PEA. The precise analysis of the proposed mechanism is conducted based on the developed model, and the optimal characteristic of the spring as well as the gear ratio are determined to generate large torque while utilizing motor torque efficiently.

In addition to this optimal design, the force controller is developed for the proposed actuator module taking into consideration the dynamic characteristic of PEA. Finally, the performance of the proposed PEA and controller are verified through experiments.

Keywords: Parallel Elastic Actuator, Force Control, Motorized Exercise Machine, Optimal Design

Contents

Abstract	i
List of Contents	iii
List of Tables	iv
List of Figures	v
1 Introduction	1
1.1 Background and Motivation	1
1.2 Contributions	2
2 Characteristic of Parallel Elastic Actuator	4
2.1 Parallel Elastic Actuator Compared with Series Elastic Actuator	4
2.2 Consideration for High Performance Parallel Elastic Actuator	6
3 Dynamic Analysis and Optimization of PEA	7
3.1 PEA Developed for Physical Exercise	7
3.2 Dynamic Model of PEA	9
3.3 Optimal Selection of Gear Ratio	10
3.3.1 Optimal Gear Ratio with Sinusoidal Load Pattern	10
3.3.2 Optimal Gear Ratio with Constant Load	11
3.4 Analysis of Spiral Spring	12
3.5 Optimal Design of Spiral Spring	14
4 Development of PEA with Optimal Gear Ratio and Spring Parameter	16
4.1 Measurement of Physical Exercise	16
4.2 Optimal Design of Spring	17
4.3 Decision of Gear Ratio	20
4.4 Capacity Comparison with Helical Torsion Spring	22

5	Torque Controller Design and Verification	23
5.1	PEA Output Torque Controller	23
5.2	Experimental Setup to Verify the Performance of the Proposed PEA	24
5.3	Spring Property Verification	24
5.4	Force Control Verification	25
6	Conclusion and Future works	29

List of Tables

1	Information of motor, reduction gear and encoder utilized in the proposed PEA	7
2	Designed parameters of spiral spring.	17
3	Table summarizing the parameters of interest	20

List of Figures

1	Comparison of the force and motion relationship in PEA and SEA	5
2	Exercise procedure using the proposed actuator module	8
3	Exploded view of the proposed actuator	8
4	Schematic of PEA dynamics	9
5	Configuration and parameters of the spiral spring. The outer diameter, arbor diameter, width and material thickness are denoted by OD, A, b, and, t, respectively	13
6	Design flow chart of the proposed actuator	15
7	Blue dashed lines and red solid lines represent encoder and load cell data and fitting graph, respectively	16
8	Blue, green and yellow areas are feasible area which satisfy the desired conditions. The red markers indicate the optimal values of width, length and outer diameter	19
9	Frequency response of the system	21
10	Red makers represent the optimal gear ratio	21
11	Block diagram of PEA output torque controller	23
12	Experiment setup for verification	24
13	Red solid lines represent the measured torques with the load cell. Blue dashed line represents the calculated torque with measured angle and 0.7955 Nm/rad	25
14	Estimation of the output torque of PEA. Blue solid line and red solid line with circle marker represent the desired torque and the estimated output torque, respectively. Yellow dashed line with diamond marker and green dashed line with square marker represent the estimated spring torque and the estimated motor torque, respectively	26
15	Blue solid lines with square marker and red dotted lines represent the desired torque and the measured output torque by load cell. Green solid lines represent the estimated spring torque	27
16	Maximum output torque verification. Black solid line and blue dotted line represent the desired torque and the measured output torque by load cell. Red dashed line shows the maximum value	28

1. Introduction

1.1. Background and Motivation

Actuators that can generate and control the desired torque have been developed aiming at various human-machine interactions [1]. Among these human-machine interaction systems, the home based exercise has been receiving a lot of attention. Home exercise is more efficient than going to the gym in terms of time and money [2, 3]. Accordingly, exercise equipment is being developed utilizing torque/force controlled actuators, which can be used for home training or exercise in non-gravity condition for astronauts because they can provide various exercise loads.

Passive elastic equipment such as rubber bands is widely utilized thanks to its advantage in terms of price and size. However, the ability of this passive exercise equipment is limited in exerting large force, and it does not provide constant force. Therefore, motorized exercise equipment has been developed to overcome this issue. A limitation of this motorized exercise equipment is that the system tends to become large as the required exercise load level is high [4, 5, 6].

Meanwhile, the flywheel exercise device (FWED) was proposed [7] as a device that provides resistance during coupled concentric and eccentric muscle actions, through the inertia of a spinning flywheel. Other advanced resistive exercise device (ARED) was proposed by NASA [8] which uses vacuum cylinders to provide resistance. These devices attempted to provide exercise load large enough while keeping the size as compact as possible.

This research proposes a novel actuator module that can generate force/torque large enough for physical exercise utilizing the electric motor. Parallel Elastic Actuator (PEA) structure is employed for this actuator module such that the spring force is also utilized to enhance the output force/torque while reducing the required motor torque. Moreover, the motor torque can be controlled in real-time to provide various level and type of exercise load.

The PEA can compensate for insufficient motor torque by connecting elastic components in parallel. Because the parallel spring can provide part of the torque required to perform the task, lowering the required motor torques. Reduction of motor torques also allow for smaller motor and gear ratio. Due to these reasons, it can increase the force that the equipment can produce while reducing the size and weight of the entire equipment [9, 10].

Wire-driven mechanism is also widely utilized for exercise equipment thanks to its advantage such as simplicity and variability. Since the wire-driven mechanism requires a small winch mechanism composed of a wire drum [11], it can be manufactured with low cost and low inertia of system [12, 13]. In exercise application, wire-driven equipment is capable of various exercises, e.g, squat, bench press, dead lift and so on.

In most cases of wire-driven exercise system, the load is generated by the weights to realize the isotonic exercise. Hence, it is necessary to prepare various types of weights to provide many weight level for many users. Motorization can change this issue since it can provide the required load by employing the force control.

In order to combine the advantages of the wire-driven system and motorization and also to keep the required motor torque small, PEA is designed and controlled in this research to provide this variable exercise load through the tension control.

1.2. Contributions

The main purpose of this study is to design a PEA with optimization of mechanical parameters and controller design based on the dynamic analysis. As explained above, the motor torque and spring torque are combined in PEA, which can be exploited to reduce the required motor torque. In addition to this advantage, optimization design method is derived in this paper to determine the optimal gear ratio and the optimal spring shape for the compact and lightweight design.

To design PEA, it is necessary to properly select a motor, a gear and an elastic component. Since the target application is the small size wire-driven exercise equipment, high torque capacity is required for the actuator, while low stiffness is required for performance at the same time. Thus, high torque capacity with low stiffness is essential for the spring design. However, it is difficult to design a spring that can overcome the limitations in lowering stiffness while increasing torque capacity [14]. The spiral spring is adopted in the proposed PEA design, since the spiral spring is known to have high torque capacity with large deformation compared with helical torsion spring [15]. Moreover, the mechanical properties of the spring are optimally designed in this research to realize high torque capacity while keeping its volume as small as possible.

The selection of the gear also plays an important role in reducing the required motor torque while

satisfying the required torque and velocity. The stiffness and the gear ratio are usually determined to minimize the peak power or energy consumption. Verstraten *et al.* designed elastic elements with the natural frequency to minimize the peak power and energy consumption [16]. Hollander *et al.* also designed elastic elements to minimize the peak power [17]. Edgar *et al.* designed the elastic elements to simultaneously minimize the peak power and energy consumption [18]. The optimal selection of the gear ratio in this paper is determined to minimize the input motor torque, taking into consideration the repetitive load pattern required for the physical exercise.

Lastly, this paper investigates the dynamic characteristic of PEA, and force/tension control algorithm is designed taking into consideration the dynamic analysis. Since the motor and spring are connected in parallel in PEA, the spring connected in parallel must be considered in order to generate the desired torque. Plooij *et al.* and Häufle *et al.* proposed clutch mechanism [9, 19] to control the engagement of the spring torque. However, this approach is a suitable for applications that require instantaneous power as the trajectory is repeated, such as the exoskeleton. For the physical exercise, this approach may not be suitable because it has to continuously generate large force. Also, the electronic clutch with high permissible torque is very large and heavy. Toxiri *et al.* used a torque sensor [10] to directly measure the total torque output by the motor and the spring and feedback it. This approach may achieve accurate torque control, but it does not fully exploit the advantage of PEA. The force/torque output of PEA is discussed in this paper with the comparison with Series Elastic Actuator (SEA), and control algorithm is proposed to control the output force/torque of PEA.

In summary, the main contributions of this study are to design a compact PEA by optimizing the reduction gear ratio as well as the spiral spring and to conduct dynamic analysis of PEA to understand and design high performance force control.

This paper is organized as follows. In Sec. 2, the dynamic characteristic of PEA is analyzed compared with SEA, then a PEA is designed in Sec. 3 with the optimal selection of the gear ratio and the optimal design process of the spring. Actual design is also discussed in Sec. 4. Finally, the controller design and its performance verification are presented in Sec. 5. Sec. 6 discusses conclusion of the research, limitation of this study and future works.

2. Characteristic of Parallel Elastic Actuator

2.1. Parallel Elastic Actuator Compared with Series Elastic Actuator

PEA consists of motor, spring and reduction gear, which is the same as Series Elastic Actuator (SEA). The characteristics of PEA and SEA can be compared utilizing the schematic shown in Figure 1, where f_m and f_s represent the motor force and the spring/transmission force, and \dot{x}_i represents the motion of a rigid body.

In SEA, two bodies are connected through a transmission, and the force is transmitted between two bodies through the transmission. Spring is usually utilized as the transmission in SEA, such that the transmission force can be calculated as follows.

$$f_s = \frac{K}{s} (\dot{x}_1 - \dot{x}_2) = T_{imp} * (\dot{x}_1 - \dot{x}_2) \quad (1)$$

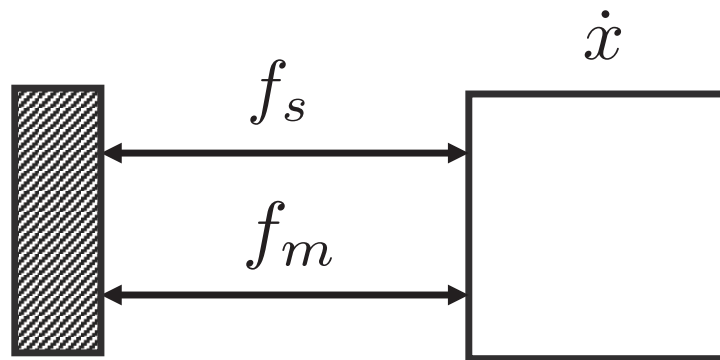
In general, the transmitted force is determined by the impedance characteristic of the transmission [20], which can be described utilizing $T_{imp}(s) = Ms + B + \frac{K}{s}$ with the mass M , the damping B and the stiffness K .

In PEA, the motion of one body \dot{x} is driven by the summation of two forces f_s and f_m , and the motion of the body is described as follows.

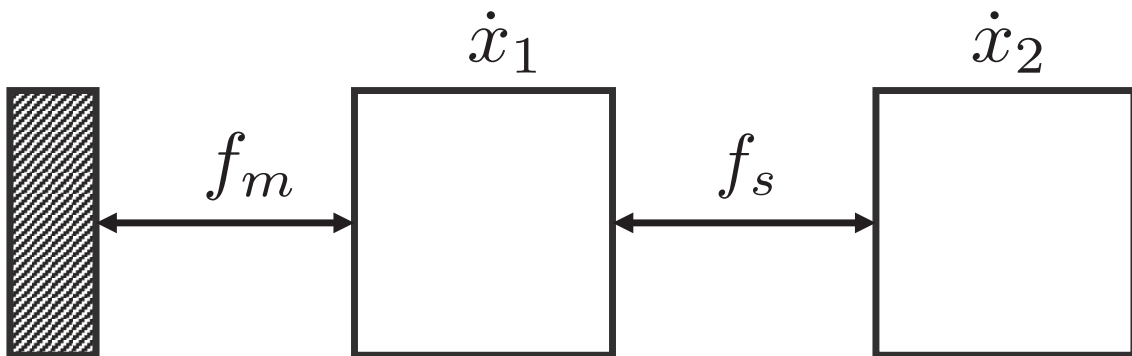
$$\dot{x} = \frac{1}{Ms} (f_m + f_s) = T_{com} * (f_m + f_s) \quad (2)$$

The equation of motion for the body can be determined by the dynamics/compliance of the body; T_{com} can be formulated as $\frac{1}{Ms+B}$ in general, where M is the mass and B is the damping. Moreover, the spring force f_s is described as $f_s = \frac{K}{s} \dot{x}$.

This comparison clarifies the characteristic of PEA. The force on the body of interest is twofold: the spring force and the motor force, while it is only the spring force in the SEA case. This is the advantage of PEA; the required force can be provided not only by the motor but also by the spring, which can reduce the required motor torque.



(a) Schematic of Parallel Elastic Actuator



(b) Schematic of Series Elastic Actuator

Figure 1: Comparison of the force and motion relationship in PEA and SEA

2.2. Consideration for High Performance Parallel Elastic Actuator

The parallel mechanism, however, can cause undesired coupling, and the range of motion (ROM) of the body is limited by the spring, which can be considered disadvantage of PEA. This is why many previous PEAs have employed the clutch mechanism; the spring needs to be detached from the main body to extend the ROM and remove the undesired coupling. Nevertheless, PEA has the advantage particularly when the desired ROM is limited and the desired motions are repetitive, e.g., suspension of vehicles and physical exercise.

To fully take advantage of PEA, several technical issues are to be addressed. Dynamic modeling of PEA plays a significant role in addressing these issues. The PEA needs to be designed in an optimal way taking into consideration its dynamic characteristics. The spring characteristics and the motor specification as well as the gear ratio can be optimally determined when its dynamic characteristics and required motion/force are known. As the ROM is limited in PEA, the gear ratio can be optimally selected in such a way the required motor torque and power are minimized.

Moreover, the coupling of PEA can be efficiently utilized when the dynamics is properly understood. Detailed analysis of PEA dynamics can clarify how the coupling affects on the PEA output force. Control algorithm can be designed to achieve high performance and effective force control of PEA based on the dynamic model.

This paper proposes solutions to these issues by presenting the dynamic analysis of PEA and the optimal design process of PEA as well as control algorithm design based on the dynamic model.

3. Dynamic Analysis and Optimization of PEA

3.1. PEA Developed for Physical Exercise

The ultimate goal of this study is to develop an actuator to provide various load for physical exercise through the wire-driven mechanism. Figure 2 illustrates exercise procedure using the proposed PEA, where the user exercises by repetitively pulling and releasing the wire that is connected to the proposed PEA. By applying this operation principle, various exercises are available such as arm curl, seated row and so on.

To allow for various exercises and exercise postures, it is necessary to adjust the point from which the spring deformation starts. To cope with this issue, a clutch mechanism is incorporated in the proposed actuator module such that the user can engage or disengage the force from the spring according to his/her preferred starting position.

The slot and saw-tooth structure are adopted to engage/disengage the wire drum from the shaft. In addition to this, an auxiliary spring is connected to the wire drum such that it can wind the wire when the user release the wire even when the main spring is disengaged. The overall design of the actuator considering these points is illustrated in Figure 3. The size of the entire actuator module is as follows: diameter and length are 120 mm and 150 mm, respectively, and the weight is 2.8 kg. The information on the components utilized in the proposed PEA module is shown in Table 1.

Table 1: Information of motor, reduction gear and encoder utilized in the proposed PEA

Component	Manufacturer	Model
Motor	HLY	X8318-KV120
Reduction gear	MATEX	75-7MLD
Encoder	Broadcom Limited	AVAGO AEDL-5810-Z12

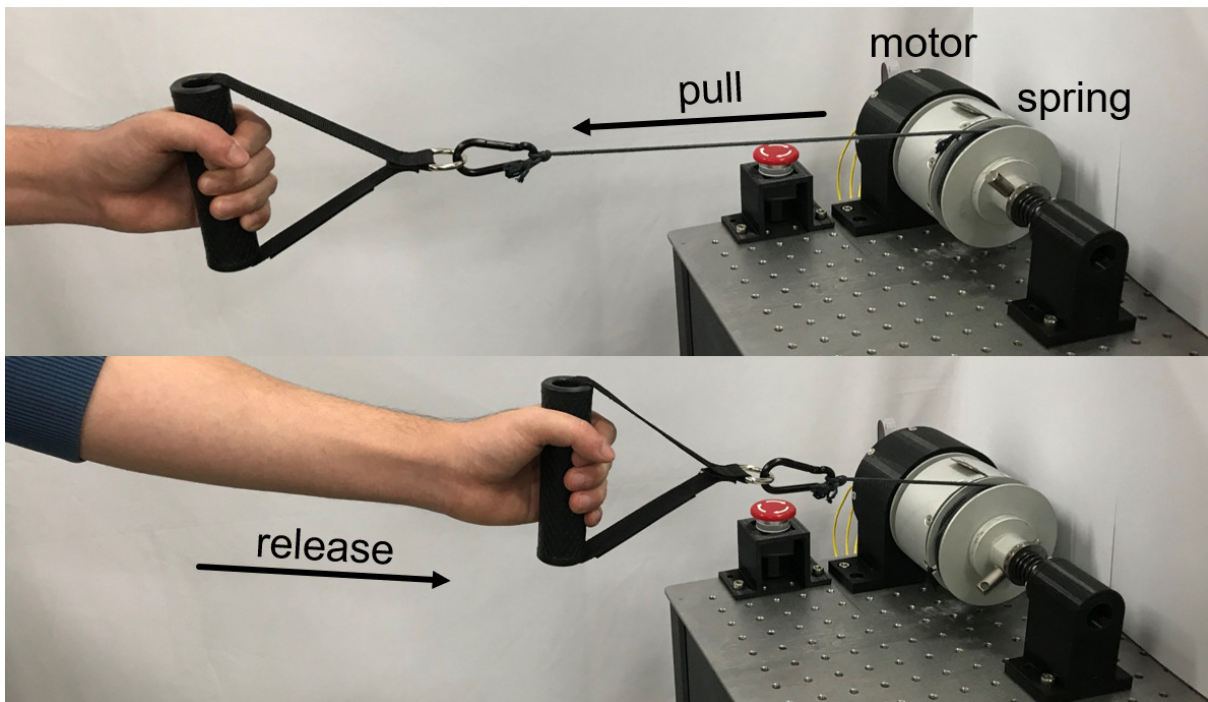


Figure 2: Exercise procedure using the proposed actuator module

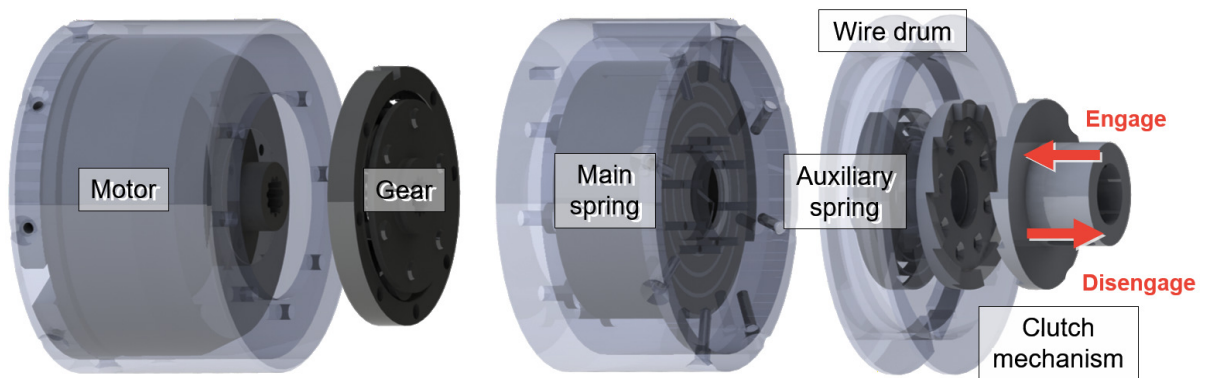


Figure 3: Exploded view of the proposed actuator

3.2. Dynamic Model of PEA

Figure 4 represents the schematic diagram of the proposed PEA. Since the PEA consists of a motor and a spring that are connected in parallel, the equation of the motor angle motion is defined as follows.

$$\tau_m = J\ddot{\theta}_m + B\dot{\theta}_m + \frac{K}{N^2}\theta_m + \frac{1}{N}\tau_{out}, \quad (3)$$

where J is the sum of the motor inertia, the gear inertia and the wire drum inertia, B is the damping coefficient, K is the stiffness of the spring, and N is the gear ratio. θ_m is the angular position of the motor, while τ_{out} is the output torque to the wire drum. As a reduction gear is employed, the relationship between the motor angular position and the wire drum angular position θ_l is given as follows.

$$\theta_m = N\theta_l \quad (4)$$

Based on this, the dynamics of (3) can be rewritten in terms of the wire drum motion as follows.

$$\tau_m = JN\ddot{\theta}_l + BN\dot{\theta}_l + \frac{K}{N}\theta_l + \frac{1}{N}\tau_{out} \quad (5)$$

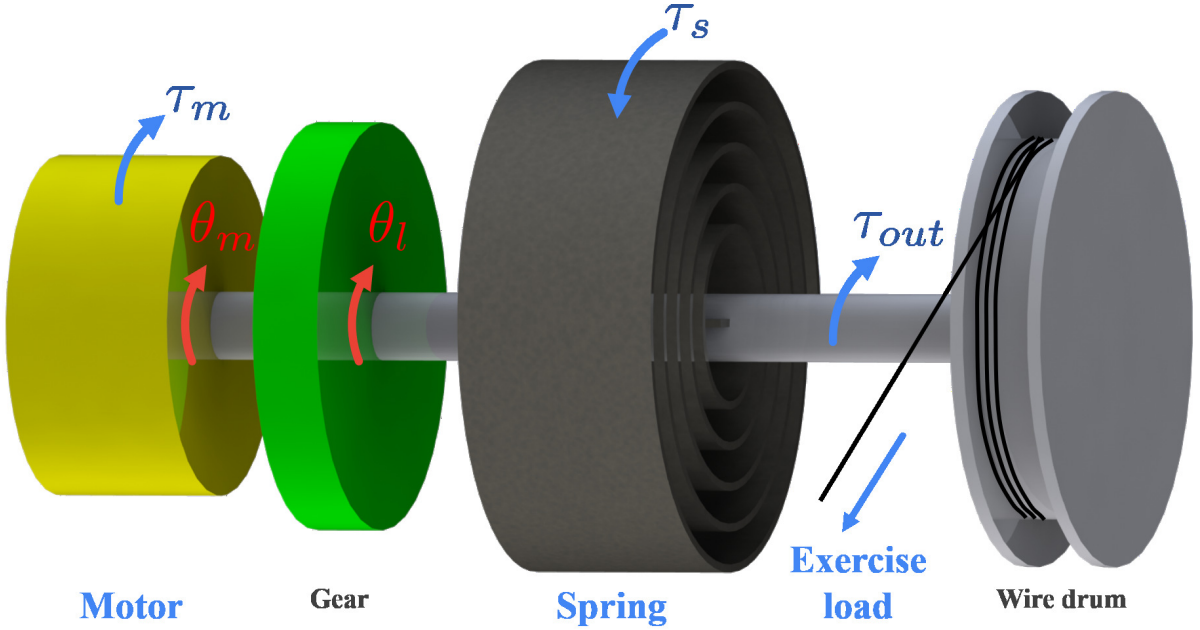


Figure 4: Schematic of PEA dynamics

3.3. Optimal Selection of Gear Ratio

Taking into consideration the derived dynamics, the gear ratio can be optimally selected. To this end, the pattern of the load angular position and the load torque trajectory are assumed to be given. This assumption is reasonable enough considering the point that there is a pattern in the exercise motion. A sinusoidal pattern is adopted for the exercise motion pattern as the exercise motion is mostly periodic. As for the load torque trajectories, two types of pattern are considered: the sinusoidal pattern and the constant value.

The objective of the optimization is to minimize the required motor torque, and thus we define the objective function and constraints as follow.

$$\begin{aligned} & \underset{N \in \mathbb{R} > 0}{\text{minimize}} && \tau_m(N) = JN\ddot{\theta}_l + BN\dot{\theta}_l + \frac{K}{N}\theta_l + \frac{1}{N}\tau_{out} \\ & \text{subject to} && \theta_l(t) = \theta_d^{max} \sin(\omega t), \\ & && \tau_{out}(t) = \tau_d^{max} \sin(\omega t) \text{ or } \tau_{out}(t) = \tau_d^{max}, \end{aligned}$$

where τ_d^{max} is the desired maximum exercise load, θ_d^{max} is the desired maximum exercise motion amplitude, and ω is the frequency of the exercise motion.

3.3.1. Optimal Gear Ratio with Sinusoidal Load Pattern

At first, the exercise motion $\theta_l(t)$ and the required exercise load $\tau_{out}(t)$ are assumed to be given as follows.

$$\theta_l(t) = \theta_d^{max} \sin(\omega t) \tag{6}$$

$$\tau_{out}(t) = \tau_d^{max} \sin(\omega t) \tag{7}$$

Then, substituting (6), (7) into (5), the peak time t_m at which the motor torque to realize the required motion and load becomes the maximum is obtained by calculating the point where $\partial\tau_m/\partial t = 0$.

$$\sqrt{\alpha^2 + \beta^2} \sin(\omega t + \phi) = 0 \tag{8}$$

$$t_m = \frac{\pi - \phi}{\omega}, \tag{9}$$

where α , β and ϕ represent as follows.

$$\alpha = -BN\theta_d^{max}\omega^2$$

$$\beta = -JN\theta_d^{max}\omega^3 + \frac{K\theta_d^{max} + \tau_d^{max}}{N}\omega$$

$$\tan(\phi) = \frac{\beta}{\alpha}$$

Then, the maximum motor torque at t_m is derived as follows.

$$\tau_m^{max} = \sqrt{\gamma N^2 + \frac{\delta}{N^2} - \epsilon}, \quad (10)$$

where γ , δ and ϵ represent as follows.

$$\gamma = (J\theta_d^{max}\omega^2)^2 + (B\theta_d^{max}\omega)^2$$

$$\delta = (K\theta_d^{max} + \tau_d^{max})^2$$

$$\epsilon = 2J\theta_d^{max}(K\theta_d^{max} + \tau_d^{max})\omega^2$$

Finally the optimal gear ratio N_{opt} which minimizes the maximum required motor torque can be obtained using the partial derivative $\partial\tau_m^{max}/\partial N = 0$. (11) is the derived optimal gear ratio.

$$N_{opt} = \sqrt[4]{\frac{\delta}{\gamma}} \quad (11)$$

Notice that the same optimization process can be applied even when there is phase difference between the exercise motion and the required load pattern.

3.3.2. Optimal Gear Ratio with Constant Load

Optimal gear ratio can be derived with the constant load torque, too. Here, the required load torque $\tau_{out}(t)$ is assumed to be constant as in (12), while the exercise motion is periodic as in (6).

$$\tau_{out,c}(t) = \tau_d^{max} \quad (12)$$

The peak time can be derived in the same way by calculating the point where $\partial\tau_m/\partial t = 0$ as in (8) and (9). However, β and ϕ in this peak time calculation becomes different from the previous case. β_c and ϕ_c that determines the peak time with the constant load are given as follows.

$$\beta_c = -JN\theta_d^{max}\omega^3 + \frac{K\theta_d^{max}}{N}\omega,$$

$$\tan(\phi_c) = \frac{\beta_c}{\alpha}$$

The maximum motor torque to realize the constant exercise load, then, is calculated utilizing α , β_c and ϕ_c , motor torque, $\tau_{m,c}^{max}$.

$$\tau_{m,c}^{max} = \sqrt{\gamma N^2 + \frac{(K\theta_d^{max})^2}{N^2} - 2JK\theta_d^{max}\omega^2 + \frac{\tau_d^{max}}{N}} \quad (13)$$

The optimal gear ratio $N_{opt,c}$ can be also obtained using the partial derivative. i.e. $\partial\tau_{m,c}^{min}/\partial N = 0$.

3.4. Analysis of Spiral Spring

The volume of the spring also needs to be minimized to design the PEA as small as possible, and the optimization of the spring shape can be conducted utilizing the property of the spiral spring. At first, the stiffness K_s of the spiral spring is determined as the division of the torque and the deformation. The deformation of the spiral spring is approximated using the bending stress model, which can be computed by the following formulas [3].

$$K_s = \frac{EbT^3}{12L} \quad (14)$$

$$S = \frac{6\tau}{bT^2}, \quad (15)$$

where K_s is the stiffness, S is the stress, E is Young's modulus, b is the width of spring strip, T is the thickness of a spiral spring, L is the length of the strip, and τ is the moment applied on the spring. The spring parameters are shown in Figure 5. Therefore, the maximum torque and deformation of the spiral spring are determined when the material and spring parameters in (14) and (15) are determined.

Meanwhile, the maximum compression angle of the spiral spring is also determined kinematically as follows.

$$\theta_{kine}^{max} = \frac{\pi(\sqrt{A^2 + 1.27LT} - A)}{T} - \frac{4L}{OD + A}, \quad (16)$$

where A is the arbor diameter, OD is the outer diameter. If the deformation exceeds this maximum compression angle, non-linearity occurs due to friction. Therefore, maximum deformation should satisfy following inequality.

$$\theta_{kine}^{max} \geq \theta^{max} \quad (17)$$

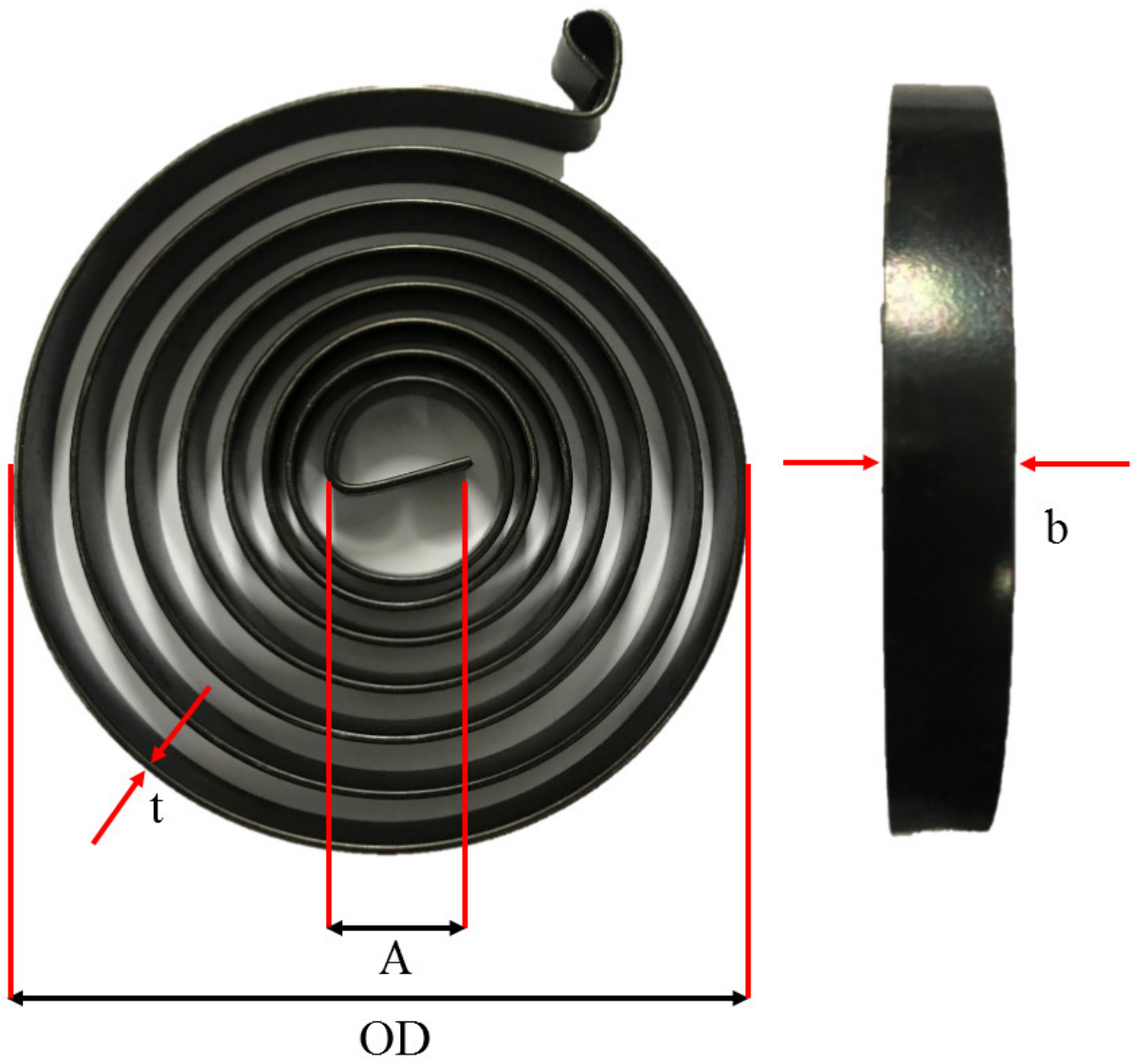


Figure 5: Configuration and parameters of the spiral spring. The outer diameter, arbor diameter, width and material thickness are denoted by OD, A, b, and, t, respectively

3.5. Optimal Design of Spiral Spring

As the objective of the spring shape optimization is to minimize the spring volume for compact actuator design, we define the objective function and the constraints using (14) and (15) as follow.

$$\begin{aligned} & \underset{T \in \mathbb{R} > 0}{\text{minimize}} && V_s(T) = \pi \left(\frac{OD(T)}{2} \right)^2 b(T) \\ & \text{subject to} && S \geq \frac{6\tau_d^{max}}{bT^2}, \\ & && \tau_d^{max} = \frac{EbT^3}{12L} \theta_d^{max}, \\ & && \theta_{kine}^{max} \geq \theta^{max} \end{aligned}$$

The relationships between the spring properties b , L , OD and T are obtained from this constraints as follows.

$$b \geq \frac{6\tau_d^{max}}{ST^2} \quad (18)$$

$$L \geq \frac{E\theta_d^{max}}{2S} T \quad (19)$$

$$OD \geq \frac{4L}{\pi(\sqrt{A^2 + 1.27LT} - A)/T - \theta_d^{max}} - A \quad (20)$$

Notice that all the properties of the spring, the width b , the length L and the outer diameter OD are the functions of the thickness T . In other words, the minimum $b(T)$ and $OD(T)$ can be obtained as follows, which can minimize the spring volume when the thickness T is given.

$$b^{min}(T) = \frac{6\tau_d^{max}}{ST^2} \quad (21)$$

$$OD^{min}(T) = \frac{4E\theta_d^{max}T^2}{\pi\sqrt{4S^2A^2 + 1.27E\theta_d^{max}T^2} - 2S(\pi A - \theta_d^{max}T)} - A \quad (22)$$

Notice that the minimum values of b^{min} and OD^{min} decrease as T increases. This relationship reveals that the volume of the spring $V_s(T)$ decreases as T increases, and there is no the optimal thickness which satisfies $\partial V_s(T)/\partial T = 0$. The thickness T , however, is usually determined based on the practical constraint such as manufacturing constraints.

In summary, the proposed optimal design process of PEA can be illustrated as in Figure 6.

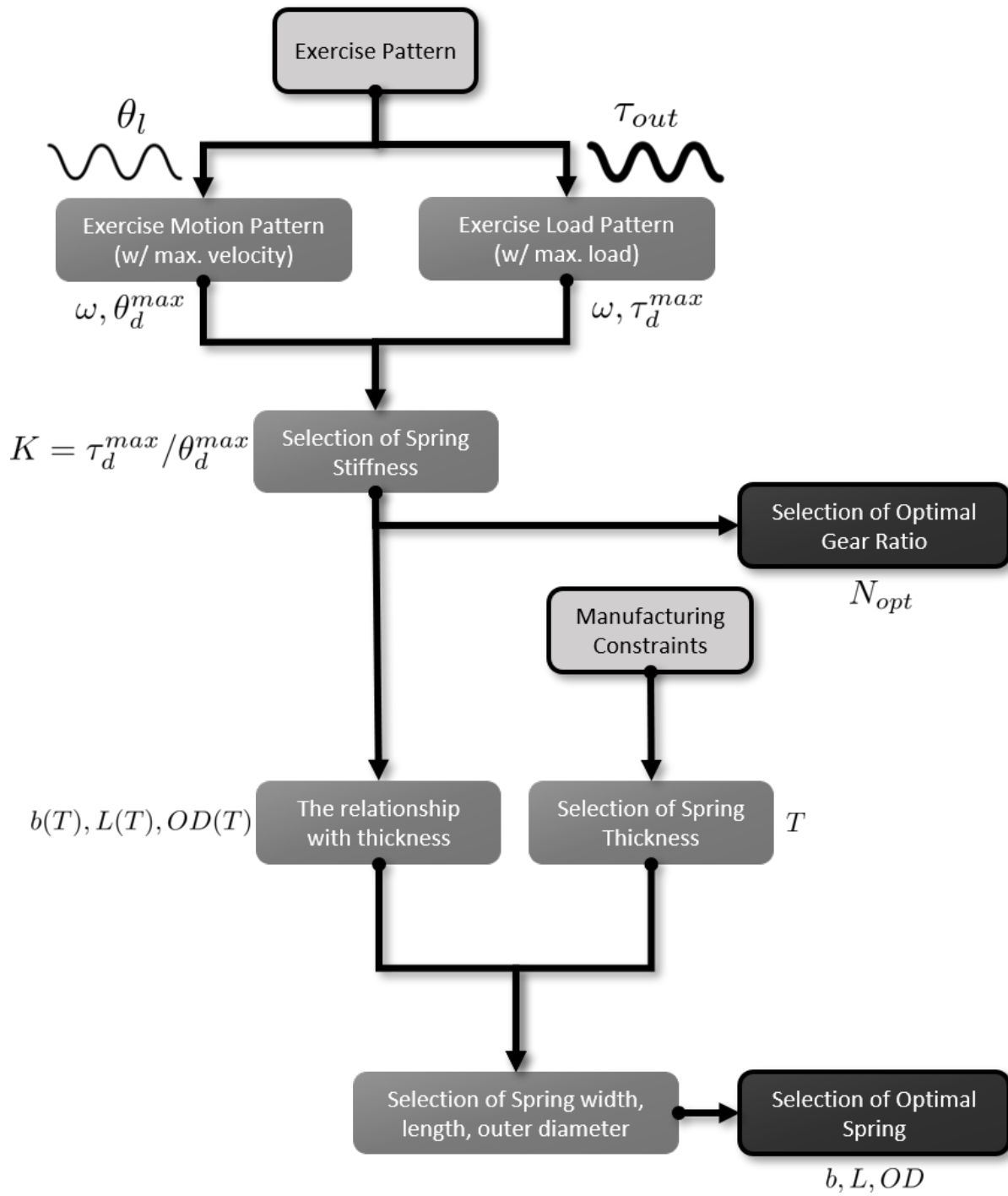
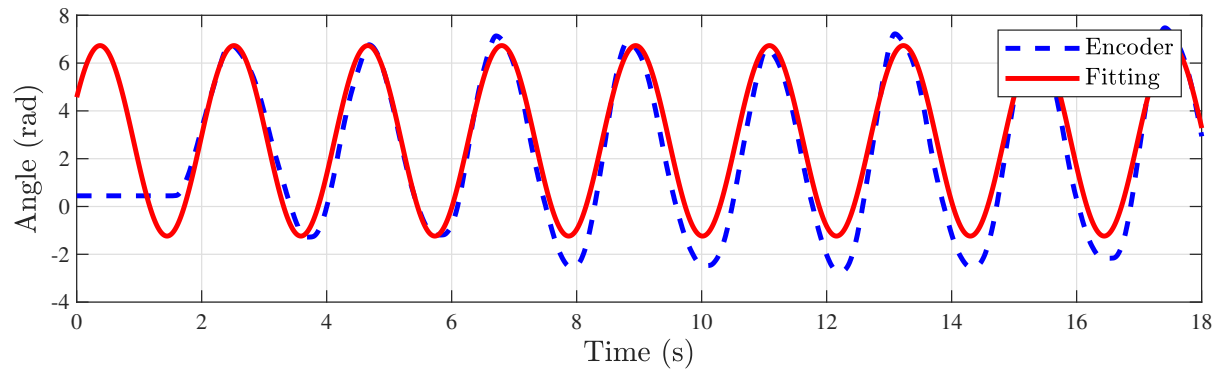


Figure 6: Design flow chart of the proposed actuator

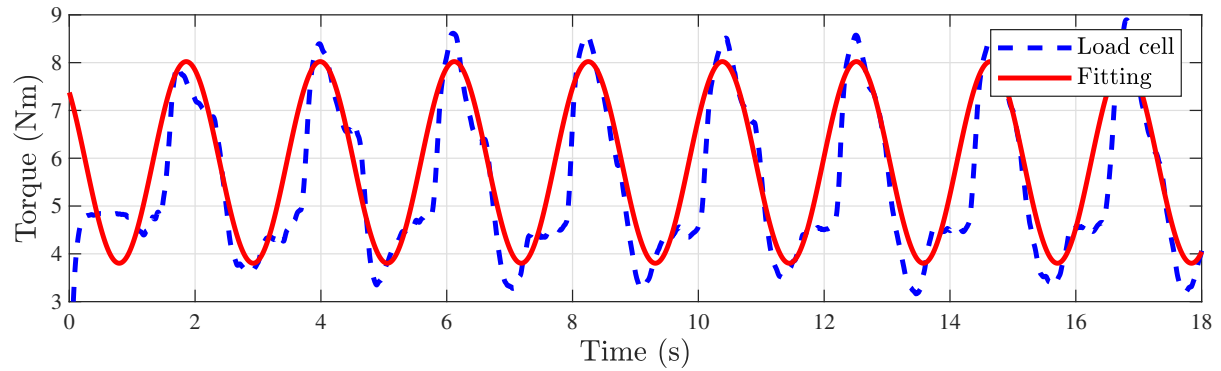
4. Development of PEA with Optimal Gear Ratio and Spring Parameter

4.1. Measurement of Physical Exercise

To choose a frequency of physical exercise, the actual physical exercise motion and load are measured. Figure 7 shows the measured motion and load. It can be found that the frequency of this exercise is around 3 rad/s, thus, ω is utilized to 3 rad/s as the exercise frequency based on which the spring and the gear ratio are optimized.



(a) Angle trajectory and fitting graph



(b) Torque trajectory and fitting graph

Figure 7: Blue dashed lines and red solid lines represent encoder and load cell data and fitting graph, respectively

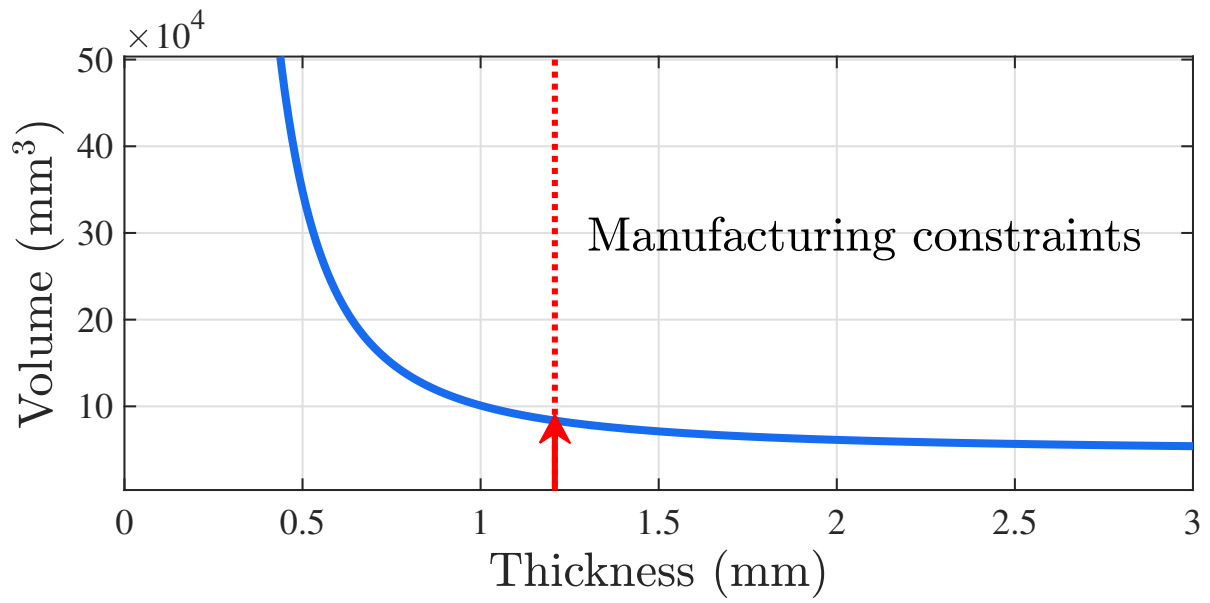
4.2. Optimal Design of Spring

For the proposed PEA design, the maximum exercise load and range of motion are set to 10 Nm and 12.57 rad, respectively. The maximum load is set to a similar level compared to the conventional motorized exercise equipment. The stiffness required for the PEA design, therefore, is derived as 0.7955 Nm/rad.

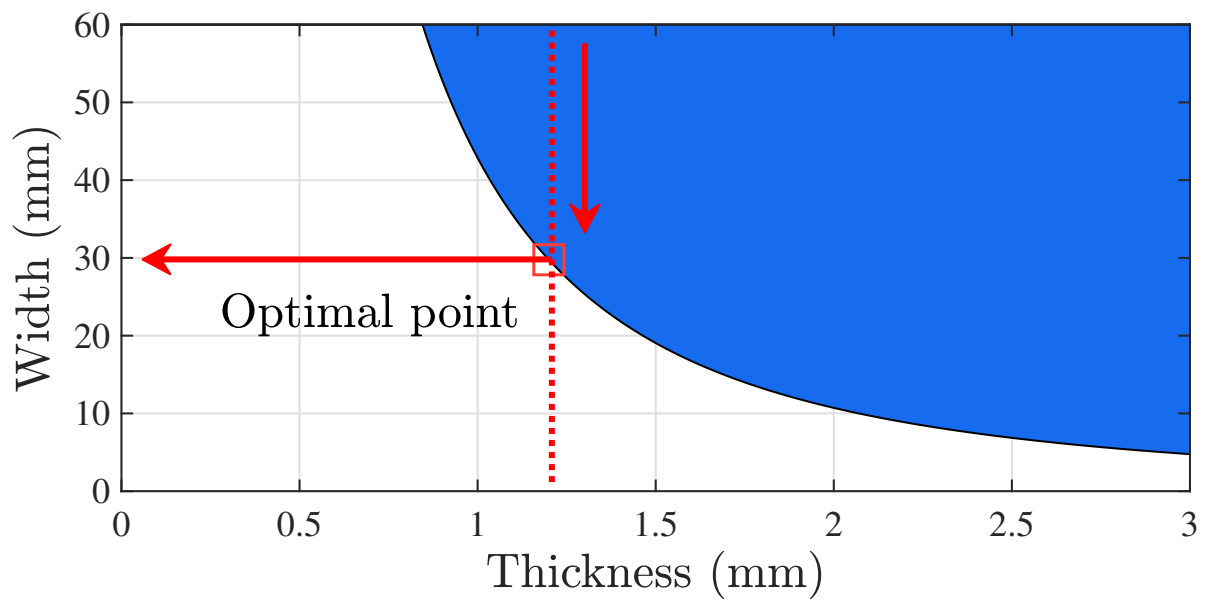
Based on this selection of stiffness, the condition for the width, the length and the outer diameter are derived using (14) to (20). Figure 8 shows the graphs which represent the spring volume, the width, the length, and the outer diameter when thickness is given. In this research, the thickness is set to 1.2 mm by manufacturing restrictions, which determines the other remaining spring properties based on (21), (22). The determined parameters are summarized in Table 2.

Table 2: Designed parameters of spiral spring.

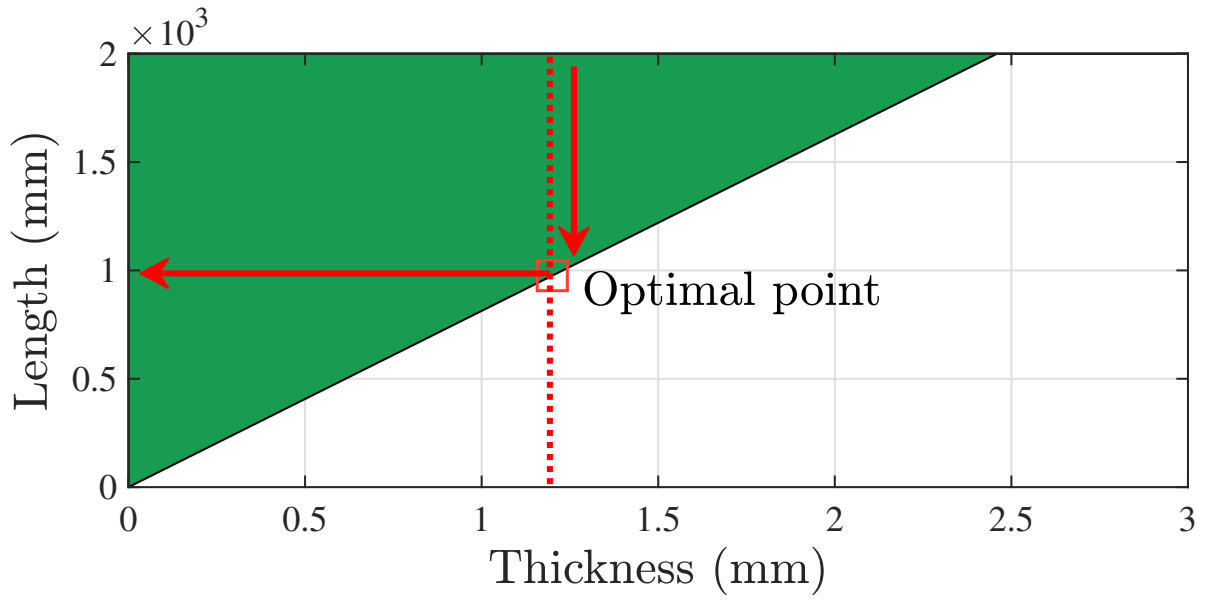
Parameter	Value
Material	Stainless steel 304
Maximum stress (S)	1,400 [MPa]
Young's modulus (E)	19.0×10^4 [MPa]
Thickness (T)	1.2 [mm]
Arbor diameter (A)	20 [mm]
Width (b)	30 [mm]
Length (L)	976 [mm]
Outer diameter (OD)	60 [mm]



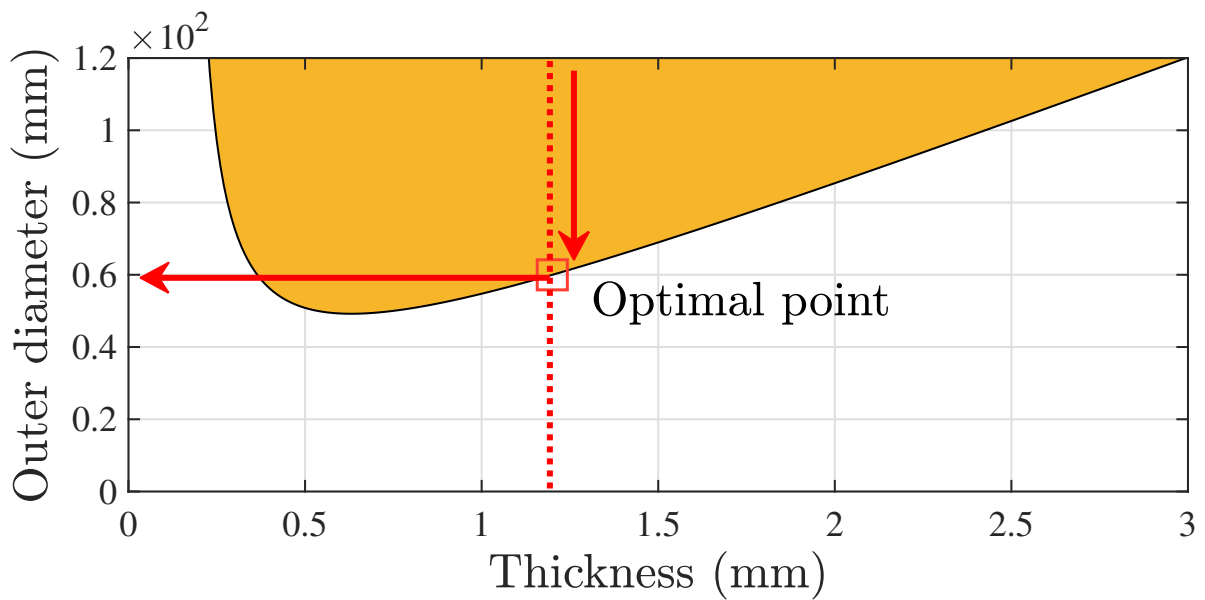
(a) Spring volume-thickness graph



(b) Width-thickness graph



(c) Length-thickness graph



(d) Outer diameter-thickness graph

Figure 8: Blue, green and yellow areas are feasible area which satisfy the desired conditions. The red markers indicate the optimal values of width, length and outer diameter

4.3. Decision of Gear Ratio

The optimal gear ratio for the proposed PEA is calculated using (11). The parameters to calculate the analytical solutions were obtained as follows: The inertia J and damping coefficient B were identified based on Empirical Transfer Function Estimation (ETFE) method [21]. Figure 9 shows the frequency response of system. Spring stiffness K are determined as 0.7955 Nm/rad in the previous subsection. Table 3 shows all the parameters utilized for the proposed PEA design.

Table 3: Table summarizing the parameters of interest

Parameter	Value
Inertia (J)	0.001099 [kgm ²]
Damping coefficient (B)	0.00665 [Nm/rad/s]
Spring stiffness (K)	0.7955 [Nm/rad]
Exercise Frequency (ω)	3 [rad/s]
Desired torque (τ_d^{max})	10 [Nm]
Desired deformation (θ_d^{max})	12.57 [rad]

The optimal gear ratio are calculated as 7.3958 and 6.8045 for the sinusoidal and the constant load patterns, respectively. Figure 10 shows how the required motor torque changes according to the gear ratio, which verifies that the derived optimal gear ratio can minimize the required motor torque for each case.

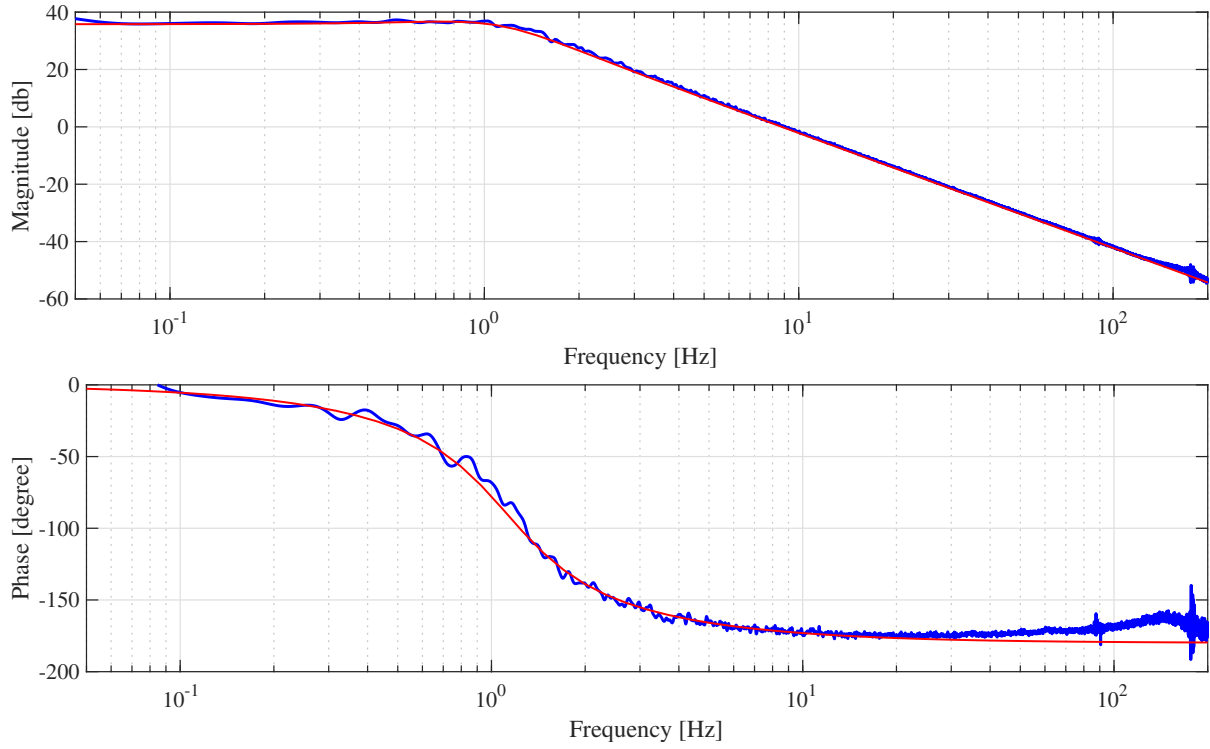
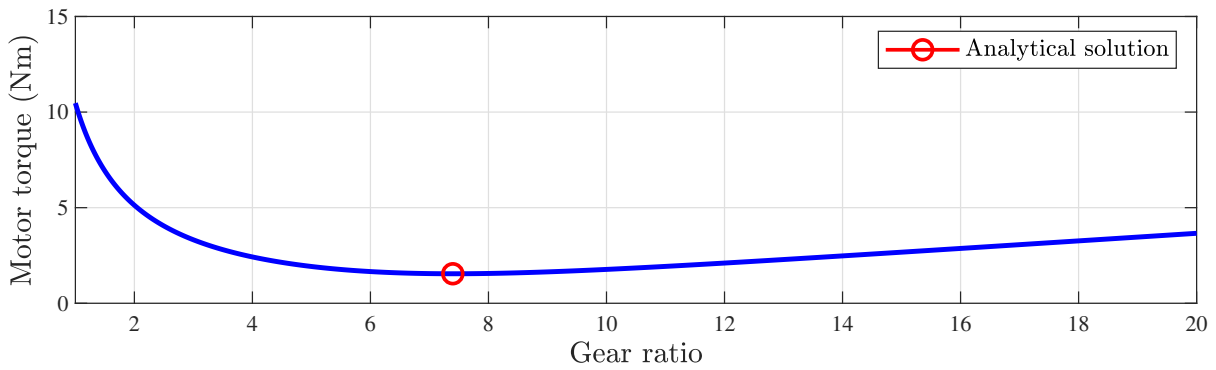
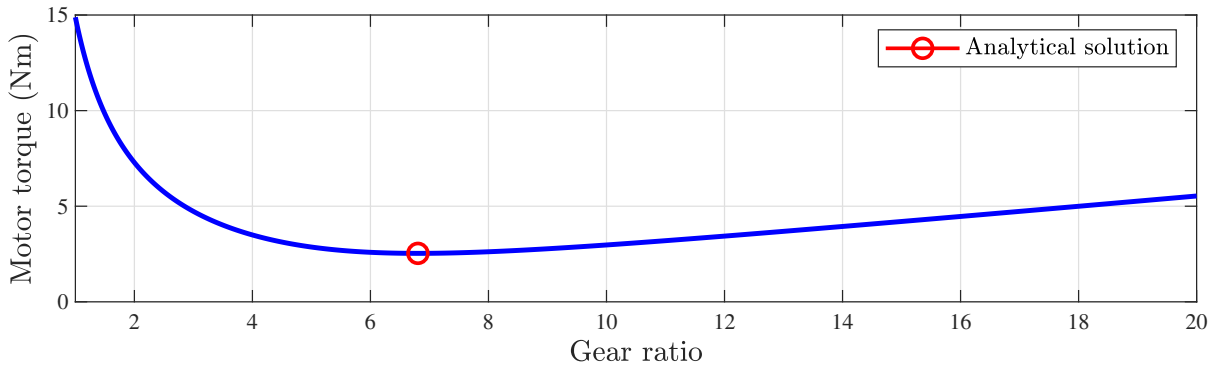


Figure 9: Frequency response of the system



(a) Required motor torque for gear ratio in sinusoidal load trajectory



(b) Required motor torque for gear ratio in constant load trajectory

Figure 10: Red makers represent the optimal gear ratio

4.4. Capacity Comparison with Helical Torsion Spring

To compare difference with spiral spring and helical torsion spring, especially the maximum deformation, helical torsion spring was analyzed. In order to compare only the maximum deformation, a spring was designed with a similar size as outer diameter is 60 mm, width is 30 mm and a similar maximum torque as 11.140 Nm. The helical torsion spring satisfies following formulas [22].

$$\tau^{max} = \frac{\pi d^3 S_y}{32 K_i}, \quad (23)$$

$$\theta^{max} = \frac{21.6\pi M_{max} D N_b}{d^4 E}, \quad (24)$$

where d is the wire diameter, S_y is the normal yield strength, K_i is the bending stress-correction factor, D is the mean diameter, N_b is the number of active coils and E is the Young's modulus. From the given, desired conditions and (24), the maximum deformation of helical torsion spring was obtained as 2.07 rad. Compared to the spiral spring, it is almost 0.167 times. As a result, helical springs with the similar size and torque capacity have much less maximum deformation capacity than that of spiral springs.

5. Torque Controller Design and Verification

5.1. PEA Output Torque Controller

One of the main purposes of our research is to generate an desired exercise load. To this end, a feedback force controller is designed to control the exercise load the user feels. The block diagram of the proposed force controller is illustrated in Figure 11.

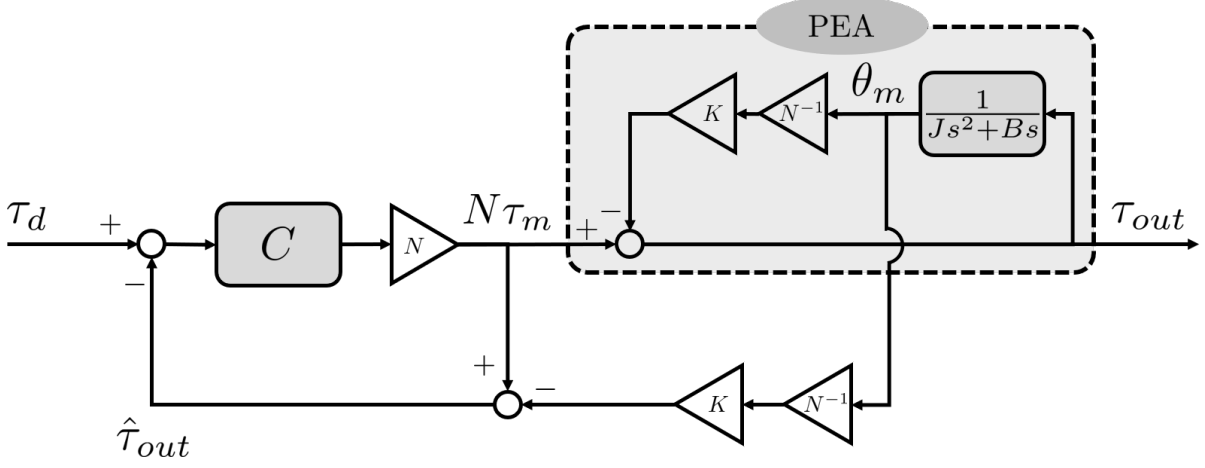


Figure 11: Block diagram of PEA output torque controller

In the proposed controller, the output torque of the PEA is defined as (25) based on the PEA dynamic model in (3) and Figure 1.

$$\tau_{out} = N\tau_m - \frac{K}{N}\theta_m \quad (25)$$

Proportional-Integral (PI) controller is designed using this output force feedback to realize the desired exercise load τ_d .

$$\tau_m^{PI} = K_p(\tau_d - \hat{\tau}_{out}) + K_i \int_0^t (\tau_d - \hat{\tau}_{out}) dt, \quad (26)$$

where K_p and K_i are the P gain and the I gain, respectively. $\hat{\tau}_{out}$ represents the output torque estimated using the relationship in (25).

5.2. Experimental Setup to Verify the Performance of the Proposed PEA

Two types of experiments are conducted to verify the spring stiffness and the force control performance of PEA. Figure 12 illustrates the experiment setup, where a load cell (CAS-SBA-50L) is attached at the end of the wire to measure the force the user feels.

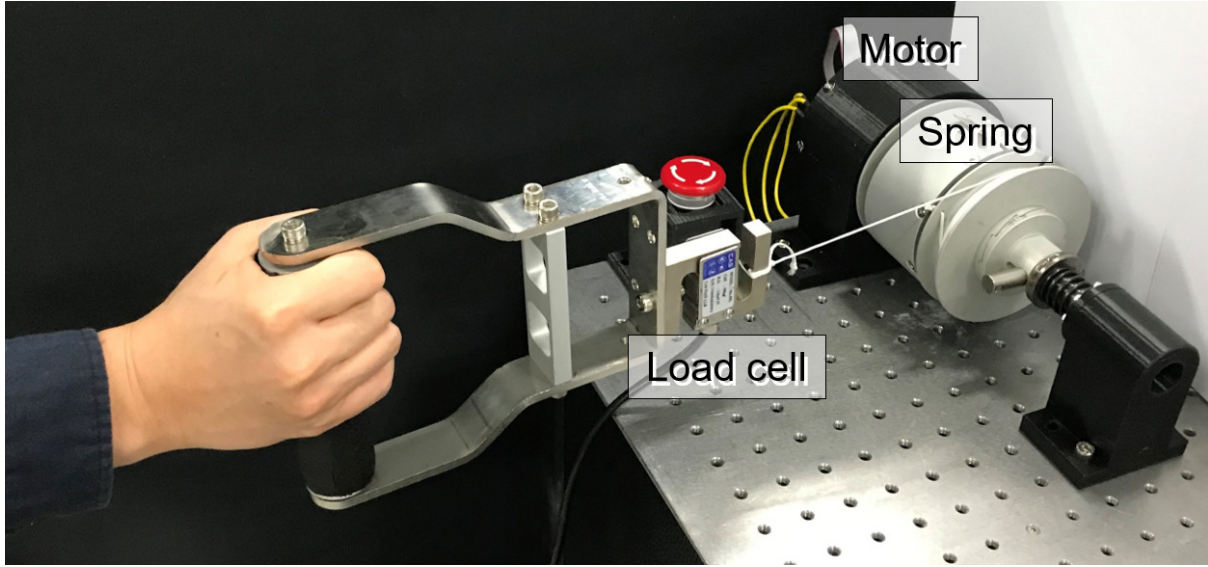


Figure 12: Experiment setup for verification

5.3. Spring Property Verification

Even though the stiffness is set to 0.7955 Nm/rad , and the spring properties T , b , L , OD are optimally designed to realize this stiffness, it should be verified whether the actual stiffness of the spring designed in this way has the desired stiffness or not.

To this end, the actual stiffness of the manufactured spring is measured through experiments. In the experiment, the wire drum is connected only to the spring (the motor is detached from the shaft), and the wire is pulled to apply the torque to spring. Wire is pulled from 0 to 12 rad in increments of 1 rad . Each angle is maintained for a constant time to confirm the static properties.

The experimental results are shown in Fig. 13. The graph plots the measured angle and the measured torque, which is the product of the load cell measurement and the radius of the drum. The measured results are compared with the theoretical relationship which has 0.7955 Nm/rad . The red lines show the measured torques for each angle, which almost matches with the ideal stiffness line.

However, as the deformation angle increases, the error tends to become larger; up to 1 Nm error occurs at 12 rad. This can be attributed to the hysteresis characteristic of the spring. Although, most of the sections show acceptable linearity as the theory.

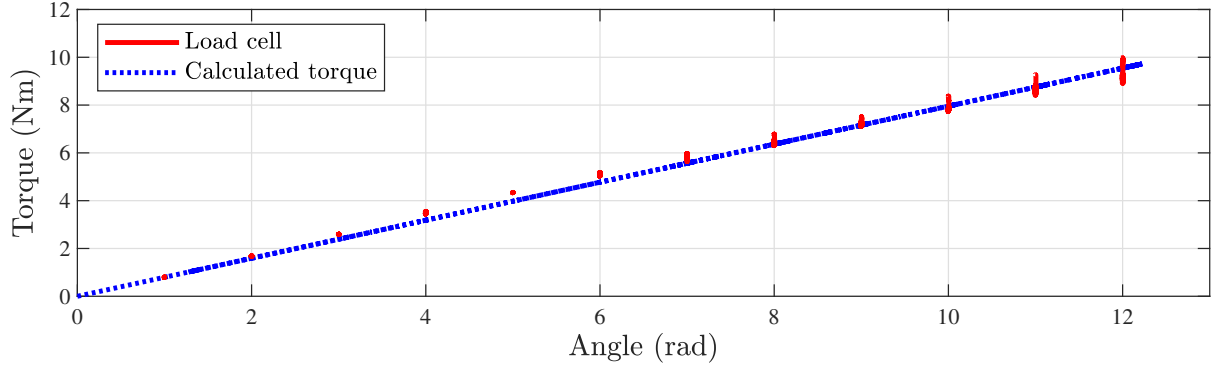


Figure 13: Red solid lines represent the measured torques with the load cell. Blue dashed line represents the calculated torque with measured angle and 0.7955 Nm/rad

5.4. Force Control Verification

The force control performance confirmed that the sum of elastic and actuator torque follows desired torque well. In other words, the goals of the experiment are, 1) to verify whether the spring can assist the insufficient torque of the motor and 2) to verify that the output torque follows the desired torque well.

In the first experiment, the desired torque is set constant, and the user conducts exercise by pulling and releasing the wire. The actual output torque is measured by the load cell, and the spring torque and the motor torque during the exercise are plotted in Figure 14.

Notice that the torque output estimated as in (25) shows similar behaviour as the desired constant torque. The difference between two can be attributed to the feedback control error and the ignored dynamic characteristic of the inertia and the damping.

Another interesting point in this experiment is that, insufficient motor torque is compensated for by the spring force. Notice that the desired torque is realized by the summation of the motor torque and the spring torque.

In the second experiment, it is shown that the output torque of the proposed PEA can be well-controlled by feedback of the estimated output torque. In the experiment, the user pulls the wire such that the wire drum angle varies from 1 rad to 4 rad and maintains the angle to verify the static characteristic.

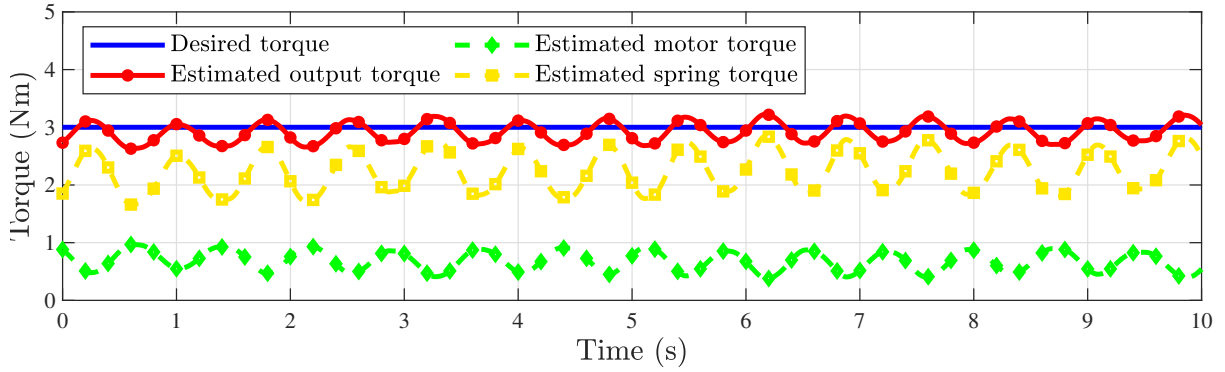
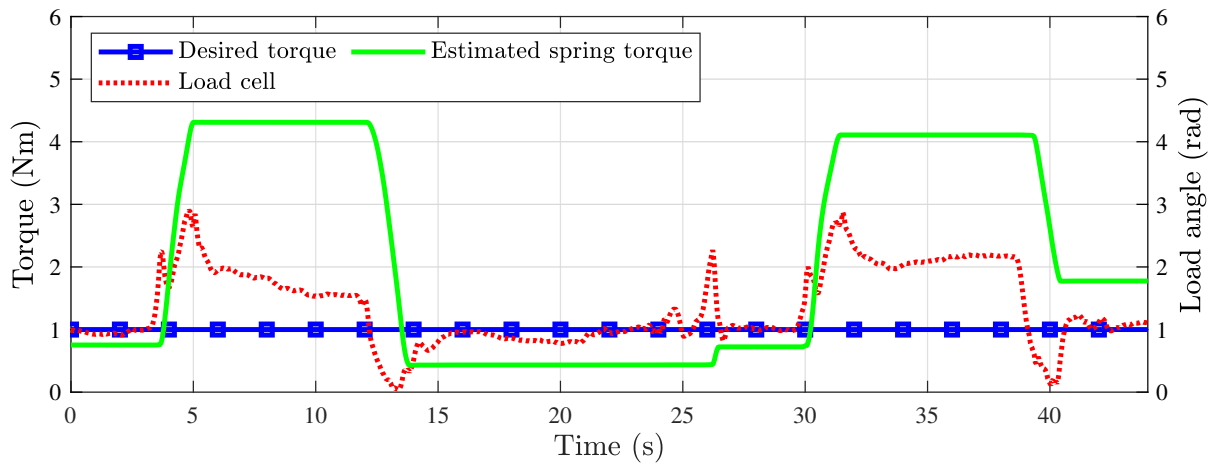


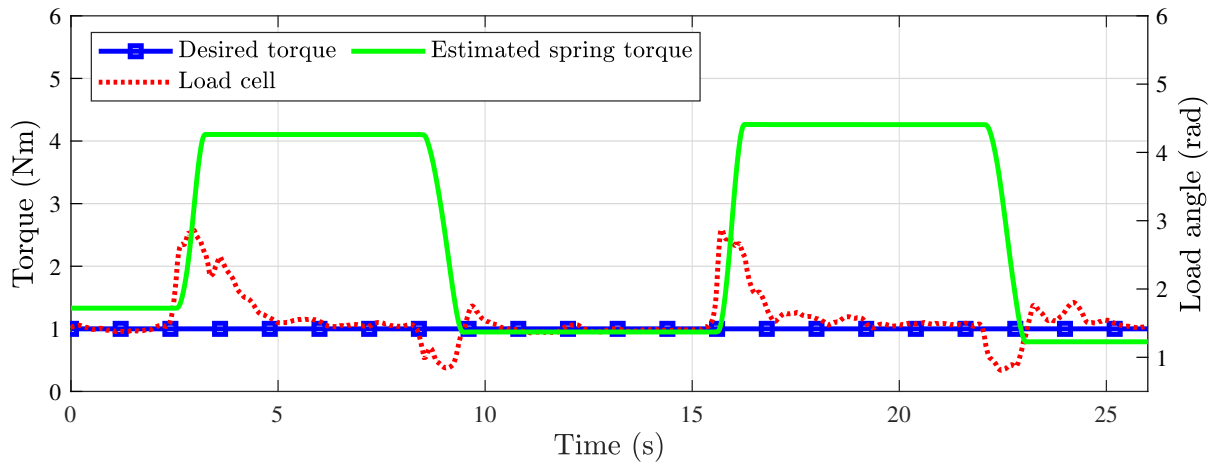
Figure 14: Estimation of the output torque of PEA. Blue solid line and red solid line with circle marker represent the desired torque and the estimated output torque, respectively. Yellow dashed line with diamond marker and green dashed line with square marker represent the estimated spring torque and the estimated motor torque, respectively

The investigate the performance of the output torque feedback controller, Proportional (P) only controller and PI controller are implemented and the results are analyzed. The desired torque level is set to 1 Nm, and the actual output torque is measured by the load cell and compared with the desired torque level.

The experimental results in Figure 15 verify that the output torque of the proposed PEA (the red dotted line) can be controlled using the estimation feedback control even with different spring deformation level. The results show that the feedback of the output torque estimation performs as expected with P and PI controllers; the steady-state error can be reduced with I controller even if the angle changes significantly. However, since dynamics characteristics such as inertia and damping term are not considered when configuring the controller, overshoot occurs significantly in the section where the angle changes.



(a) P controller tracking result under angle variation



(b) PI controller tracking result under angle variation

Figure 15: Blue solid lines with square marker and red dotted lines represent the desired torque and the measured output torque by load cell. Green solid lines represent the estimated spring torque

In the third experiment, it is shown the maximum output torque that the actuator can generate by using the designed controller. In the experiment, the user pulls the wire while increasing the desired torque to 20 Nm that the actuator can generate.

The investigate the performance of the maximum output torque, the results are analyzed. The desired torque level is up to 14 Nm, and the actual output torque is measured by the load cell and compared.

The experimental results in Figure 16 verify that the maximum output torque of proposed PEA (the blue dotted line) can generate 14 Nm.

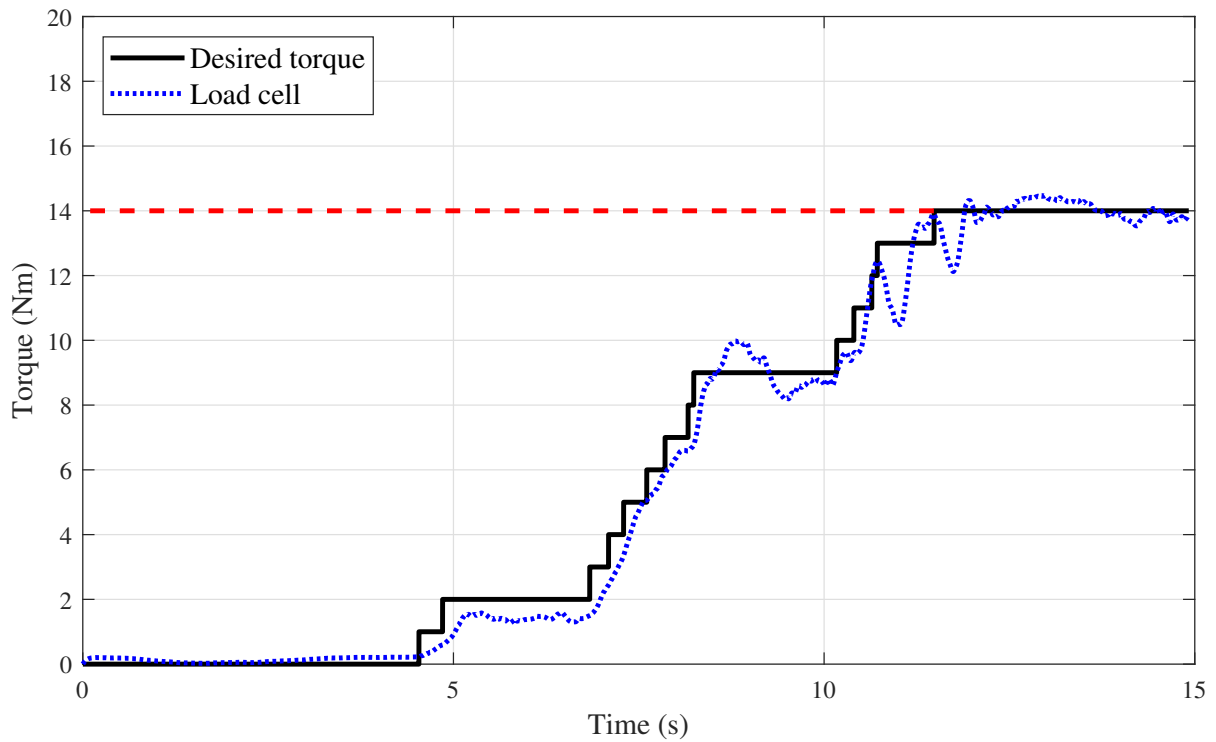


Figure 16: Maximum output torque verification. Black solid line and blue dotted line represent the desired torque and the measured output torque by load cell. Red dashed line shows the maximum value

6. Conclusion and Future works

This paper proposed a novel parallel elastic actuator that can generate force for physical exercise. The PEA mechanism can compensate for insufficient motor torque by connecting the spring in parallel. This characteristics allows a smaller motor to be used, resulting in reduction in size and weight of the actuator. Although a PEA has the disadvantage that ROM is limited, it works as an advantage in physical exercises that require limited ROM and repeated motions. Therefore, it is suitable for exercise applications.

To maximize these strengths and achieve research goals, optimization methodology and controller design based on dynamics were proposed. The optimization contributes to designing a compact and lightweight design actuator, and the controller design contributes to generating the desired exercise load for the PEA to function as an exercise equipment.

The result of the optimization, the entire weight of the actuator is only 2.8 kg. Compared to the first unoptimized actuator, it is 0.4 kg heavier, but the torque it can generate is 10 Nm larger.

However, there are limitations and future works. When designing the actuator, the maximum torque that the motor and spring can generate were assumed to be the same for convenience of control. There is insufficient verification as to whether this assumption is optimal. It is necessary to analyze this assumption because the ROM and the maximum torque of the actuator are changed according to the ratio of the maximum torque between the motor and the spring. In addition, as the gear ratio increases, the parameter value varies accordingly in gear ratio optimization. This study didn't consider the effect of this factor. Finally, compensation for friction and dynamic characteristics was not applied to the controller. This affects the performance of force control. Therefore, it is necessary to design a controller that consider these factors.

References

- [1] H. Vallery, J. Veneman, E. Van Asseldonk, R. Ekkelenkamp, M. Buss, H. Van Der Kooij, Compliant actuation of rehabilitation robots, *IEEE Robotics & Automation Magazine* 15 (3) (2008).
- [2] F. J. Penedo, J. R. Dahn, Exercise and well-being: a review of mental and physical health benefits associated with physical activity, *Current opinion in psychiatry* 18 (2) (2005) 189–193.
- [3] A. Spring, *Design handbook: Engineering guide to spring design*, Associated Spring, Barnes Group Inc., 1981, pp. 181–184.
- [4] Y. Ping, S. Shuang, H. Lei, et al., Resistive exercise device based on spring mechanism for astronauts, *Journal of Mechanical Engineering* 50 (23) (2014) 1–7.
- [5] K. L. English, J. A. Loehr, M. A. Laughlin, S. Lee, R. D. Hagan, Reliability of strength testing using the advanced resistive exercise device and free weights (2008).
- [6] L. Zhang, L. Li, Y. Zou, K. Wang, X. Jiang, H. Ju, Force control strategy and bench press experimental research of a cable driven astronaut rehabilitative training robot, *Ieee Access* 5 (2017) 9981–9989.
- [7] D. Hueser, C. Wolff, H. E. Berg, P. A. Tesch, M. Cork, The fly wheel exercise device (fwd): A countermeasure against bone loss and muscle atrophy, *Acta Astronautica* 62 (2-3) (2008) 232–239.
- [8] J. A. Loehr, S. M. Lee, K. L. English, J. Sibonga, S. M. Smith, B. A. Spiering, R. D. Hagan, Musculoskeletal adaptations to training with the advanced resistive exercise device, *Medicine & Science in Sports & Exercise* 43 (1) (2011) 146–156.
- [9] M. Plooi, M. Wisse, H. Vallery, Reducing the energy consumption of robots using the bidirectional clutched parallel elastic actuator, *IEEE Transactions on Robotics* 32 (6) (2016) 1512–1523.
- [10] S. Toxiri, A. Calanca, J. Ortiz, P. Fiorini, D. G. Caldwell, A parallel-elastic actuator for a torque-controlled back-support exoskeleton, *IEEE Robotics and Automation Letters* 3 (1) (2017) 492–499.
- [11] P. Gallina, 23 wire driven robots for rehabilitation, in: *Advances in Rehabilitation Robotics*, Springer, 2004, pp. 365–375.

- [12] V. Vashista, A cable-driven pelvic robot: Human gait adaptation and rehabilitation studies, Ph.D. thesis, Columbia University (2015).
- [13] Y. Mao, X. Jin, G. G. Dutta, J. P. Scholz, S. K. Agrawal, Human movement training with a cable driven arm exoskeleton (carex), *IEEE Transactions on Neural Systems and Rehabilitation Engineering* 23 (1) (2014) 84–92.
- [14] R. Van Ham, T. G. Sugar, B. Vanderborght, K. W. Hollander, D. Lefeber, Compliant actuator designs, *IEEE Robotics & Automation Magazine* 16 (3) (2009) 81–94.
- [15] Y. Kim, J. Lee, J. Park, Compliant joint actuator with dual spiral springs, *IEEE/ASME Transactions on Mechatronics* 18 (6) (2013) 1839–1844.
- [16] T. Verstraten, P. Beckerle, R. Furnémont, G. Mathijssen, B. Vanderborght, D. Lefeber, Series and parallel elastic actuation: Impact of natural dynamics on power and energy consumption, *Mechanism and Machine Theory* 102 (2016) 232–246.
- [17] K. W. Hollander, R. Ilg, T. G. Sugar, D. Herring, An efficient robotic tendon for gait assistance (2006).
- [18] E. A. B. Nieto, S. Rezazadeh, R. D. Gregg, Minimizing energy consumption and peak power of series elastic actuators: a convex optimization framework for elastic element design, *IEEE/ASME Transactions on Mechatronics* 24 (3) (2019) 1334–1345.
- [19] D. F. Häufle, M. Taylor, S. Schmitt, H. Geyer, A clutched parallel elastic actuator concept: Towards energy efficient powered legs in prosthetics and robotics, in: 2012 4th IEEE RAS & EMBS International Conference on Biomedical Robotics and Biomechanics (BioRob), IEEE, 2012, pp. 1614–1619.
- [20] Y. Park, N. Paine, S. Oh, Development of force observer in series elastic actuator for dynamic control, *IEEE Transactions on Industrial Electronics* 65 (3) (2018) 2398–2407. doi:10.1109/TIE.2017.2745457.
- [21] L. Ljung, State of the art in linear system identification: Time and frequency domain methods, in: *Proceedings of the 2004 American Control Conference, Vol. 1*, IEEE, 2004, pp. 650–660.

- [22] R. G. Budynas, J. K. Nisbett, et al., Shigley's mechanical engineering design, Vol. 8, McGraw-Hill
New York, 2008, pp. 515–520.

요약문

장력제어를 위한 병렬 탄성 구동기의 최적화 설계

본 논문은 장력제어를 이용하여 운동부하를 생성하는 어플리케이션을 위한 병렬 탄성 구동기의 최적화 설계에 대해서 다룬다. 병렬 탄성 구동기는 모터에 스프링을 병렬로 연결한 구동기로, 구동기에서 내고자 하는 토크 중 일부를 스프링이 내주어 모터가 내야할 토크를 줄여줄 수 있는 장점이 있다. 이러한 장점은 결과적으로 모터와 기어의 크기를 줄이는 효과를 주어 더 작고 가벼운 형태의 구동기를 만들 수 있게 한다. 하지만 최적설계를 위해서는 스프링과 기어의 선정이 주요한데, 본 논문에서는 태엽스프링과 기어비 최적화 방법론을 제안했다. 먼저 태엽스프링은 기존에 많이 사용하는 helical torsion spring과 비교했을 때 비슷한 크기와 토크 능력을 가진다고 가정했을 때, 태엽스프링이 더 큰 변형량을 가질 수 있는 특성이 있다. 이러한 특성은 해상도를 높여 제어 성능면에서 더 유리하며, 다양한 운동에 더 적합하다는 장점을 가지고 있다. 두 번째로 기어 최적화 방법론은 기어비가 커짐에 따라 기어비의 크기와 무게도 비례하여 커지기 때문에 필요한 토크 수준에 맞는 적절한 기어비의 선정이 필요하다. 이를 위해 주어진 모션과 토크 trajectory를 가정하여 최적의 기어비를 선정하였다. 두 가지 방법론을 통해 설계한 스프링과 기어비를 바탕으로 최적의 병렬 탄성 구동기를 설계 및 제작하였다. 추가적으로, 본 논문에서는 이를 검증하기 위해 제어기를 구성하였다. 구동기의 성능을 실험을 통해 확인하였다. 그 결과, 비슷한 수준의 무게이지만 훨씬 더 큰 힘을 낼 수 있는 구동기를 개발하였다.

핵심어: 병렬 탄성 구동기, 장력제어, 최적 설계, 모터라이즈 운동 기구